

A fatigue driving energy approach to high-cycle fatigue life estimation under variable amplitude loading

Z. PENG, H-Z. HUANG, S-P. ZHU, H. GAO and Z. LV

Institute of Reliability Engineering, University of Electronic Science and Technology of China, No. 2006, Xiyuan Avenue, West High-tech Zone, Chengdu, Sichuan 611731, China

Received Date: 13 February 2015; Accepted Date: 15 July 2015; Published Online: 26 August 2015

ABSTRACT In this paper, a concept of fatigue driving energy is formulated to describe the process of fatigue failure. The parameter is taken as a combination of the fatigue driving stress and strain energy density. By assessing the change of this parameter, a new non-linear damage model is proposed for residual life estimation within high-cycle fatigue regime under variable amplitude loading. In order to consider the effects of loading histories on damage accumulation under such condition, the load interaction effects are incorporated into the new model, and a modified version is thus developed. Life predictions by these two models and Miner rule are compared using experimental data from literature. The results show that the proposed model gives lower deviations than the Miner rule, while the modified model shows better prediction performances than the others. Moreover, the proposed model and its modifications are ease of implementation with the use of S–N curve.

Keywords high-cycle fatigue; life estimation; non-linear damage model; strain energy density; variable amplitude loading.

NOMENCLATURE

A	= fatigue strength constant
b	= material constant
D	= damage variable
E	= Young's modulus
h	= fatigue strength exponent
n	= number of cycles at a given stress level
N_f	= number of cycles to failure
W	= elastic strain energy density
W_a	= amplitude of elastic strain energy density
W_D	= fatigue driving energy
W_{D_0}	= initial fatigue driving energy
W_{D_c}	= critical fatigue driving energy
σ	= applied load stress level
σ_D	= fatigue driving stress
σ_{equiv}	= equivalent fatigue driving stress
σ_a	= applied stress amplitude
σ_f	= fatigue strength coefficient
ε	= elastic strain
ε_a	= elastic strain amplitude
ω	= interaction factor

INTRODUCTION

In engineering applications, fatigue failure is prevalent and prone to be one of the most common failure modes

Correspondence: H.-Z. Huang, E-mail: hzhuang@uestc.edu.cn

for most engineering components, which are usually subjected to cyclic loading. During their service operation, fatigue loading often involves variable amplitude loading (VAL), yet seldom constant amplitude loading (CAL). The concept of damage is crucial to describe

the process of fatigue failure, and it also plays an important role in fatigue life estimation. Owing to the complex loading histories, assessing the fatigue damage behavior of these components depends on special testing under actual service conditions, which is costly and time consuming. In contrast, testing under CAL is more readily implemented and very cost-effective, and these available CAL data contribute to evaluate the fatigue damage under VAL. However, loading histories effects, such as load sequences, load interactions, etc., have a significant influence on damage evolution. Therefore, there is a strong need to develop a reliable model to deal with the process of damage accumulation under variable fatigue loading, aiming to enable a better estimation of fatigue life.

Until now, many damage accumulation models have been developed for fatigue life estimation. One of the most commonly used models is the Palmgren–Miner rule¹ (Miner rule or linear damage rule) because of its simplicity and ease of implementation in design. Fatigue failure is expected to occur when the cumulative damage is equal to the critical cumulative damage, i.e. unity. Unfortunately, the model is acknowledged to be overshadowed by its intrinsic shortcomings,^{2,3} shown as:

- (1) In the case of CAL, the Miner rule is load-level independent, and the damage evolution process remains the same for any given stress level.
- (2) In the case of VAL, each stress level keeps the relative independence, regardless of load interactions and load sequences accountability.
- (3) The model is exclusive of the fatigue damage induced by small loads below the fatigue limit.

In addition, many studies^{4–8} suggest that Miner rule is inaccurate or gives a large deviation with the reality for certain combinations of variable loading. Some researchers endeavour a lot to modify it, but life estimates using these extended versions are still found to be unsatisfactory.³ The inadequacy may be typically attributed to the model itself. Subsequently, to address the intrinsic deficiencies associated with the Miner rule, researchers have resorted to the non-linear cumulative damage theories, and various non-linear versions are developed.^{3,9,10}

Essentially, fatigue damage is a process of irreversibility, material properties degradation and energy dissipation. It is essential to the definition of a reliable damage model when quantifying and accumulating fatigue damage. In general, fatigue damage can be measured by assessing the changes in mechanical properties or physical properties.¹¹ For mechanical properties, a series of state variables, such as modulus of elasticity, static toughness, stiffness, ductility, reduction of area, tensile strength,

etc., are often used to characterize fatigue damage. Belaadi et al.¹² and Zhou et al.¹³ suggested that the modulus of elasticity for different materials gradually decreased with the accumulation of fatigue damage. Ye and Wang¹⁴ demonstrated that the reduction in static toughness of materials was a useful parameter to present the damage variable. Devulder et al.¹⁵ presented that the stiffness degradation could be used as a damage measure. Cheng and Plumtree¹⁶ and Zhu et al.¹⁷ showed that the reduction in ductility was suitable for assessing fatigue damage. Zhu et al.¹⁸ and Yuan et al.¹⁹ reported that the strength degradation of materials could be defined as fatigue damage. For physical properties, some state variables, such as electric, magnetic and thermal properties, are also used to characterize fatigue damage accumulation behavior. Lemaitre and Dufailly²⁰ presented that damage could be measured by the variation in the electrical potential for conductive materials. Sun et al.²¹ used the relative increment in electrical resistance to describe damage. Khonsari et al.^{11,22–24} proved that the thermodynamic entropy generation could be treated as a degradation process for damage prediction.

Ultimately, as aforementioned, these changes of material properties can be taken as the response of stress or strain indirectly.^{11,25} To a certain extent, they may be extremely attributed to the change of energy in materials. Azadi et al.²⁶ also suggested that fatigue damage monotonously increased with the accumulation of the plastic strain energy.

Recently, the strain energy density parameter has often been used for fatigue analysis. Lagoda^{27,28} gave an elaboration of the strain energy density models, which were used to estimate fatigue life under uniaxial random loading. Park et al.²⁹ proposed a strain energy density based model to describe the fatigue behavior of rolled AZ31 magnesium alloy, which shows an agreement between the predictions and the experimental data. Djebli et al.³⁰ used the strain energy density parameter to present damaged stress, while also obtaining a new version of the damaged stress model previously by Aid et al.⁷ for high-cycle fatigue life prediction. Zhu et al.³¹ developed a generalized fatigue–creep damage model on the basis of plastic strain energy density parameter, providing a better life prediction of turbine disk alloys (GH4133). In this regard, the strain energy density parameter offers an effective method to track damage accumulation behavior.

Currently, Kwofie and Rahbar³² proposed a concept of fatigue driving stress, and residual fatigue life can be estimated by determining the equivalent fatigue driving stress as the previous stress levels under VAL. However, the equivalent fatigue driving stress does not mean the equivalent fatigue damage because of the idea of equal damage introduced by Richart and Newmark.³³

In this paper, a concept of fatigue driving energy (FDE) is introduced to present fatigue damage evolution within the high-cycle fatigue regime. It is considered that the FDE is taken as a combination of the fatigue driving stress and strain energy density. By assessing the change of FDE parameter, a new non-linear damage model, as well as its modified version considering load interactions, is formulated to predict residual fatigue life under VAL. Five categories of experimental data in literature are used to investigate the applicability and capability of new models. Furthermore, a comparison with the commonly used Miner rule is also made.

A NEW NON-LINEAR DAMAGE MODEL BASED ON FDE PARAMETER

For high-cycle fatigue, the controlling parameter is significantly dependent on elastic strain or stress level. The constitutive relation between stress and life can be presented by the Wöhler curve (S–N curve), and its exponential notation can be expressed as:

$$\sigma N_f^{-b} = A \tag{1}$$

where N_f is the number of cycles to failure at a given stress level σ ; b is a constant associated with material property ($b < 0$) and A is the fatigue strength constant, which presents the inherent nature of the material independent of applied loads. Once the stress (the left side of Eq. (1) in the material with the accumulated cycles reaches the constant value A , failure or fracture occurs.

Lately, a concept of fatigue driving stress was proposed by Kwofie and Rahbar³² on the basis of S–N curve. It can be expressed as a function of applied stress, consumed life fraction and fatigue life of the applied stress, shown as:

$$\sigma_D = \sigma N_f^{-b \frac{n}{N_f}} \tag{2}$$

where n is the number of loading cycles at a given stress level σ , n/N_f is the consumed life fraction and σ_D is fatigue driving stress, which increases with the accumulated cycles until a critical value is attained, where the final fracture occurs. In the case of VAL, let the previous stress levels yield the equivalent driving stress equal to the last one, the residual life or life fraction can be achieved.

For a two-level block loading, let the stress level σ_1 be applied n_1 cycles first, followed by the stress level σ_2 applied n_2 cycles up to failure, and let N_{f1} and N_{f2} be the fatigue lives of applied stress levels, respectively.

According to Eq. (2), the estimation of residual life fraction at σ_2 can be obtained by

$$\frac{n_2}{N_{f2}} = \left(1 - \frac{n_1}{N_{f1}}\right) \frac{\ln N_{f1}}{\ln N_{f2}} \tag{3}$$

In Eq. (2), for the initial state ($n/N_f=0$), note that the fatigue driving stress depends on the applied stress only; for the critical state ($n/N_f=1$), the fatigue driving stress is a constant equal to the fatigue strength of the material, i.e. A . Plots of σ_D versus n/N_f for two different stress amplitudes (σ_1 and σ_2 , $\sigma_1 > \sigma_2$) under CAL are shown in Fig. 1. However, particularly for a low–high loading sequence (the first applied stress is σ_2 for n_2 cycles, followed by σ_1 for n_1 cycles to failure), suppose that the consumed life fraction at the lower stress level is small enough, it will cause a near impossibility of finding an available equivalent fatigue driving stress corresponding to the higher stress level (see Fig. 1, σ_{equiv} denotes the equivalent fatigue driving stress), hindering its implementation for residual life prediction.

Early in 1948, Richart and Newmark³³ introduced the concept of equal damage based on S–N approach. Up to now, residual life assessment is often implemented by the equivalent damage rule. Despite the availability of σ_{equiv} , it is always unable to guarantee that the applied stresses can yield the equivalent fatigue damage in accordance with the equivalent driving stress (except when $\sigma_{equiv} = A$). Thus, it is necessary to develop an available damage model, in terms of the equivalent damage rule, to assess residual fatigue life.

Recently, the strain energy density, generally expressed as a function of stress σ and strain ε , is often used as a damage parameter for damage calculation and

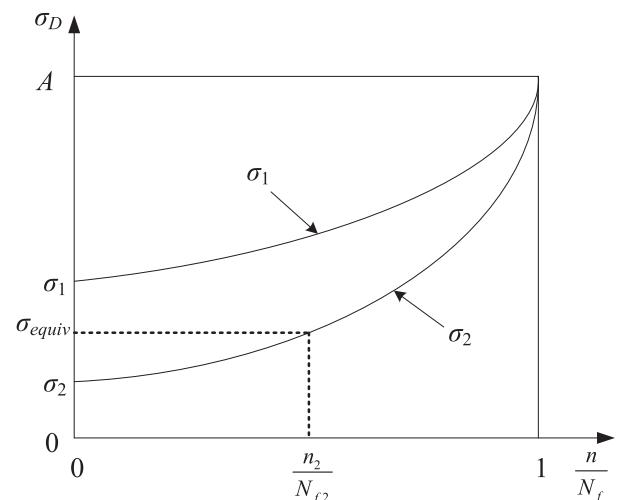


Fig. 1 Variation of fatigue driving stress under CAL for two different stress amplitudes (σ_1 and σ_2).

fatigue analysis. In the elastic range, the strain energy density parameter can be calculated in a mathematical form,²⁷ shown as:

$$W = \frac{1}{2} \sigma \varepsilon. \tag{4}$$

Then, the amplitude of this parameter can be derived as a function of stress amplitude and strain amplitude, i.e. σ_a and ε_a respectively,^{27,28,30} shown as:

$$W_a = \frac{1}{2} \sigma_a \varepsilon_a. \tag{5}$$

For high-cycle fatigue, located in the elastic range, there is a significant linear correlation between the stress and strain, expressed by the Basquin equation and Manson–Coffin equation (regardless of plastic strain) respectively, shown as:

$$\sigma_a = \sigma'_f (2N_f)^b \tag{6}$$

$$\varepsilon_a = \frac{\sigma'_f}{E} (2N_f)^b \tag{7}$$

where σ'_f is the fatigue strength coefficient, b is fatigue strength exponent and E is Young's modulus.

Substituting Eqs. (6) and (7) into Eq. (5) leads to

$$W_a = \frac{1}{2E} \sigma_a^2. \tag{8}$$

Combining Eqs. (2) and (8), a new parameter of fatigue driving energy, W_D , is expressed as follows:

$$W_D = \frac{1}{2E} \sigma^2 N_f^{-2b \frac{n}{N_f}} \tag{9}$$

For the initial state without damage, i.e. $n/N_f=0$, the FDE is

$$W_{D_0} = \frac{1}{2E} \sigma^2. \tag{10}$$

For the critical state, i.e. $n/N_f=1$, it is

$$W_{D_c} = \frac{A^2}{2E}. \tag{11}$$

Note that the initial value W_{D_0} , depending on the applied stress level, denotes the initial FDE, which attempts to cause damage in the material, while the critical value W_{D_c} , a constant with respect to the fatigue strength of the material, can be taken as the inherent energy stored in material as well as a threshold for preventing the material from failure. With regard to Eq. (9), the intermediate variable W_D , driving fatigue damage, will increase non-linearly with the accumulated

cycles until the threshold W_{D_c} is reached when the final fracture occurs.

Admittedly, fatigue damage accumulation arises from the energy dissipation in materials, which can be equal to the continuous increase of FDE up to the threshold W_{D_c} . Hence, the increment of W_D can be used to present the process of fatigue damage evolution, and a new damage accumulation model is defined as:

$$D = \frac{W_D - W_{D_0}}{W_{D_c} - W_{D_0}} = \frac{N_f^{-2b \frac{n}{N_f}} - 1}{N_f^{-2b} - 1}. \tag{12}$$

In Eq. (12), at the first cycle, the instantaneous FDE is identical to the initial value W_{D_0} , i.e. $D=0$; at the last cycle, it equals the critical value W_{D_c} and thus $D=1$. The model relates to three fitting parameters, i.e. fatigue life at the applied load (N_f), consumed life fraction (n/N_f) and material constant (b). In addition, it shows a non-linear (exponential) correlation between D and n/N_f , and the damage function relies on the fatigue life at the applied load, that is load-level dependence.

For a simply two-level block loading (at the first stress level σ_1 for n_1 cycles, then at the second stress level σ_2 for n_2 cycles to failure), according to the equivalent damage rule, the estimation of residual life fraction for σ_2 can be obtained as:

$$\left(\frac{n_2}{N_{f2}}\right)_{pp} = 1 - \frac{1}{-2b \ln N_{f2}} \tag{13}$$

$$\ln \left(\frac{\left(N_{f2}^{-2b} - 1 \right) \left(N_{f1}^{-2b \frac{n_1}{N_{f1}}} - 1 \right)}{N_{f1}^{-2b} - 1} + 1 \right)$$

where the subscript *pp* refers to the prediction by the proposed model.

Interestingly, suppose that $N_f^{-2b} \gg 1$, Eq. (12) can be rewritten as:

$$D \approx \left(\frac{1}{N_f}\right)^{-2b} \left(1 - \frac{n}{N_f}\right). \tag{14}$$

According to the equivalent damage rule, the predicted residual life fraction at σ_2 can be derived as:

$$\frac{n_2}{N_{f2}} = \left(1 - \frac{n_1}{N_{f1}}\right) \frac{\ln N_{f1}}{\ln N_{f2}} \tag{15}$$

The result is the same as Eq. (3). It indicates that the fatigue driving stress model, as shown in Eq. (2), is just a particular case of the proposed model Eq. (12) when $N_f^{-2b} \gg 1$.

Similarly, for a three-level block loading, let the third stress level σ_3 yield the equivalent damage equal to the sum of those by the previous stress levels. Then, the estimation of n_3/N_{f3} at σ_3 can be given by:

$$\left(\frac{n_3}{N_{f3}}\right)_{pp} = 1 - \frac{1}{-2b \ln N_{f3}} \ln \left(\frac{\left(N_{f3}^{-2b} - 1\right) \left(N_{f2}^{-2b \left[\frac{n_2}{N_{f2}} + 1 - \left(\frac{n_2}{N_{f2}}\right)_{pp} \right]} - 1 \right)}{N_{f2}^{-2b} - 1} + 1 \right) \tag{16}$$

It is worth noting that Eq. (16) can be easily generalized into multi-level block loading; let the stresses $\sigma_1, \sigma_2, \sigma_3, \dots, \sigma_i$ orderly be applied the number cycles of $n_1, n_2, n_3, \dots, n_i$, and let $N_{f1}, N_{f2}, N_{f3}, \dots, N_{fi}$ be the failure lives of these applied stresses, respectively. Let the cumulative damage caused by all of the previous stresses be equal to that by the last one. Thus, the estimation of n_i/N_{fi} at σ_i can be derived as:

$$\left(\frac{n_i}{N_{fi}}\right)_{pp} = 1 - \frac{1}{-2b \ln N_{fi}} \ln \left(\frac{\left(N_{fi}^{-2b} - 1\right) \left(N_{f(i-1)}^{-2b \left[\frac{n_{i-1}}{N_{f(i-1)}} + 1 - \left(\frac{n_{i-1}}{N_{f(i-1)}}\right)_{pp} \right]} - 1 \right)}{N_{f(i-1)}^{-2b} - 1} + 1 \right) \tag{17}$$

Note that Eqs. (13), (16) and (17) relate to the parameters, that is fatigue lives of applied stresses and material constant b in Eq. (1). Hence, residual life fraction can be easily obtained using S–N curve.

MODIFICATIONS AND TYPICAL BEHAVIORS OF THE PROPOSED NON-LINEAR RULES

A modified model accounting for load interactions

Generally, in the case of VAL, loading histories, such as load sequences and load interactions, have a significant effect on fatigue damage evolution. Fatigue damage variable D with a non-linear fatigue behavior is commonly formulated regarding the applied stress and the consumed life fraction. Thus, a general description of D can be presented as a function:

$$D = f\left(\sigma, \frac{n}{N_f}\right) \tag{18}$$

where D should be limited to $0 \leq D \leq 1$.

Many studies^{34–38} implied that fatigue damage evolution under VAL differed from that under CAL, the prior loading histories at a certain stress could affect the damage accumulation law by the subsequent stress. Specifically, for high–low loading sequence, it tends to accelerate the process of damage evolution at the subsequent stress, on the contrary for low–high loading sequence. Simultaneously, the bigger difference between the applied stress levels, the greater effect it shows. This phenomenon (load interactions) is commonly described in a manner of load ratio (interaction factor), reported by Corten and Dolan,³⁹ Freudenthal and Heller,³⁴ Morrow³⁵ and Huang *et al.*^{19,38,40}

As aforementioned, considering a two-level loading (n_1 cycles at σ_1 followed by n_2 cycles at σ_2 to failure), the phase of damage evolution at the first stress σ_1 remains the same as its original evolution law under CAL, while the phase at the second stress σ_2 will change. In this study, assuming that the load ratio between two successive stress levels is used as an interaction factor to present load interactions. For simplicity, the interaction factor, which is taken as a parameter ω for later convenience, can be postulated as $\omega = \sigma_1/\sigma_2$. Despite the change of damage accumulation law at σ_2 , the damage variable D with respect to n/N_{f2} should still be limited to $0 \leq D \leq 1$ during the entire life independently. As a consequence, a modified damage variable considering load interactions for σ_2 can be defined as follows:

$$D = \left[f\left(\sigma_2, \frac{n}{N_{f2}}\right) \right]^\omega = \left[f\left(\sigma_2, \frac{n}{N_{f2}}\right) \right]^{\frac{\sigma_1}{\sigma_2}} \tag{19}$$

For the proposed model, according to the equivalent damage rule, a new prediction of residual life fraction at σ_2 can be calculated by:

$$\left(\frac{n_2}{N_{f2}}\right)_{mp} = 1 - \frac{1}{-2b \ln N_{f2}} \tag{20}$$

$$\ln \left(\left(N_{f2}^{-2b} - 1 \right) \left(\frac{N_{f1}^{-2b \frac{n_1}{N_{f1}} - 1}}{N_{f1}^{-2b} - 1} \right)^{\frac{\sigma_2}{\sigma_1}} + 1 \right)$$

where the subscript *mp* refers to the prediction by the modified model.

Similarly, for three-level block loading, a new estimation of n_3/N_{f3} at σ_3 is

$$\left(\frac{n_3}{N_{f3}}\right)_{mp} = 1 - \frac{1}{-2b \ln N_{f3}}$$

$$\ln \left(\left(N_{f3}^{-2b} - 1 \right) \left(\frac{N_{f2}^{-2b \left[\frac{n_2}{N_{f2}} + 1 - \left(\frac{n_2}{N_{f2}} \right)_{mp} \right]} - 1}{N_{f2}^{-2b} - 1} \right)^{\frac{\sigma_1 \times \sigma_3}{\sigma_2}} + 1 \right). \tag{21}$$

Also, for multi-level block loading, a new estimation of n_i/N_{fi} at σ_i is

$$\left(\frac{n_i}{N_{fi}}\right)_{mp} = 1 - \frac{1}{-2b \ln N_{fi}}$$

$$\ln \left(\left(N_{fi}^{-2b} - 1 \right) \left(\frac{N_{f(i-1)}^{-2b \left[\frac{n_{i-1}}{N_{f(i-1)}} + 1 - \left(\frac{n_{i-1}}{N_{f(i-1)}} \right)_{mp} \right]} - 1}{N_{f(i-1)}^{-2b} - 1} \right)^{\frac{\sigma_{i-2} \times \sigma_i}{\sigma_{i-1}}} + 1 \right). \tag{22}$$

Notice that in Eqs. (20), (21) and (22), the prediction of residual life fraction relates to the parameters, i.e. the material constant *b* in Eq. (1), the applied stresses and their fatigue lives. These parameters can also be determined from the S–N curve.

Typical behaviors of the proposed non-linear rules under two-level fatigue loading

Two-level fatigue loading is commonly used as a representative to analyse the typical behaviours of fatigue damage rules. In order to present the significance of the proposed non-linear damage rules, three different applied loads are chosen as a demonstration of high-cycle fatigue regime, their fatigue lives are

$N_f=100\,000$, $N_f=333\,333$ and $N_f=1\,000\,000$, respectively. Besides, four typical values of material constant *b* are adopted, i.e. -0.050 , -0.250 , -0.550 and -0.950 . Consider that the initial life fraction and residual life fraction at the first and second stress loading are n_1/N_{f1} and n_2/N_{f2} , respectively. Six combinations of fatigue lives (in the form of N_{f1}/N_{f2}) are 0.3, 0.333 and 0.1 for high–low loading and 3.333, 3 and 10 for low–high loading, respectively.

Plots of n_2/N_{f2} versus n_1/N_{f1} for the selected values of *b* and all combinations of fatigue lives are shown in Fig. 2. In the figure, the following non-linear behaviours can be noted:

(1) The proposed method Eq. (13) and its modification Eq. (20) yield different fatigue envelopes dependent on the loading sequences, while Miner rule always gives the same envelope (a black straight line in Fig. 2). It suggests that Miner rule is load sequence independent; these two models developed consider the load sequence effects.

(2) The high–low and low–high fatigue envelopes lie in the left and right side of Miner’s envelope, respectively. These two envelopes exhibit some symmetry with respect to the Miner’s envelope.

(3) Either the high–low envelope or low–high envelope deviates from the Miner’s envelope with the decrease of the material constant *b*. If *b* tends to 0, these two envelopes become very close to the Miner’s envelope. As the absolute value of *b* increases, the fatigue envelopes using Eq. (20) show a significant difference with the Miner’s envelope gradually. However, all the envelopes of these two proposed non-linear rules are confined by the box from (0, 0) to (1, 1).

EXPERIMENTS AND DISCUSSIONS

In this section, five categories of experimental data, including aluminium alloy Al-2024,^{7,41} welded aluminium alloy joints of Electric Multiple Units,⁴² spheroidal graphite cast-iron (GS61),⁷ aluminium alloy 6082T6,^{7,30} and titanium alloy Ti–6Al–4V,⁴³ are used to verify the effectiveness of the proposed model, discussed in the Section on A New Non-linear Damage Model Based on FDE Parameter, and the modified model, discussed in the Section on A Modified Model Accounting for Load Interactions. Comparisons among the Miner rule, the proposed model and the modified model are made to show their prediction performances.

Case 1: aluminium alloy Al-2024

The material in this case is the aluminium alloy Al-2024.^{7,41} The experiments were carried out under two-level block loading for both low–high and

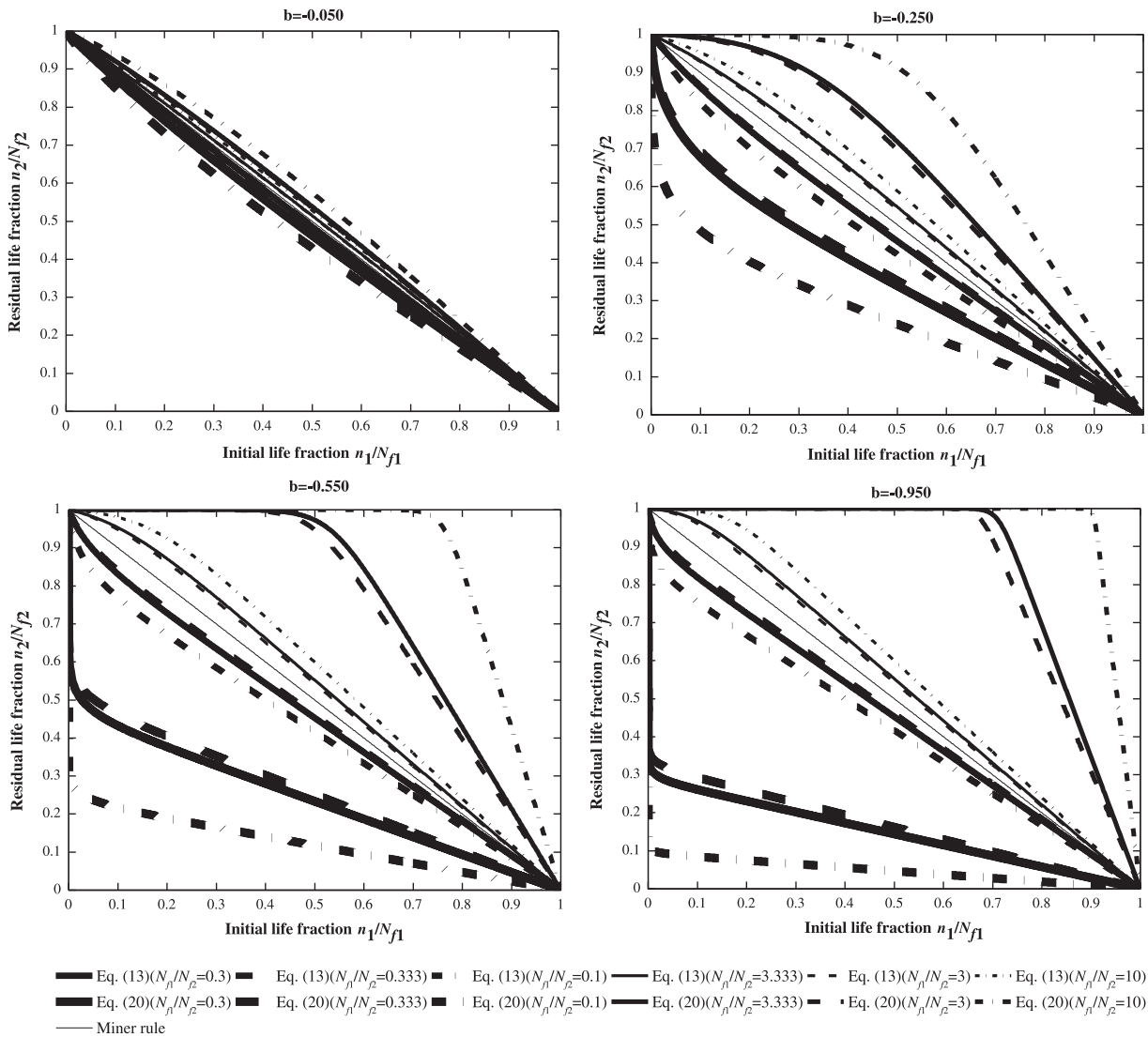


Fig. 2 Plots of residual life fraction n_2/N_{f2} versus initial life fraction n_1/N_{f1} for four typical values of b and all combinations of fatigue lives.

high–low sequences, whose load spectrums are 150–200 Mpa and 200–150 Mpa, respectively. Fatigue lives for these two applied stresses $\sigma=150$ Mpa and $\sigma=200$ Mpa are $N_f=430\,000$ cycles and $N_f=150\,000$ cycles, respectively.

In Table 1, it shows the experimental data and predicted results of the residual life fraction at the second stress level σ_2 . It can be seen that all the predictions obtained by the proposed model and the modified model agree well with the experimental data; these two presented models predict $n_1/N_{f1} + n_2/N_{f2} > 1$ for low–high loading sequence and $n_1/N_{f1} + n_2/N_{f2} < 1$ for high–low loading sequence, while Miner rule predicts $n_1/N_{f1} + n_2/N_{f2} = 1$ for each loading sequence. In Fig. 3, it also unfolds a clear comparison between the

experimental data and predicted results using these three models. It is worth noting that the proposed model predicts better results than the Miner rule, while the modified model shows a significant improvement in prediction performance over other two models.

Case 2: butt weld joint and fillet weld joint

The welded aluminium alloy joints of Electric Multiple Units are used in this study,⁴² including butt weld joint and fillet weld joint. For butt weld joint, the experimental results were obtained by two-level block loading up to the failure, three stress levels were applied for both low–high and high–low loading sequences; four configurations of load spectrums are 104–74 Mpa and 89–74 Mpa for

Table 1 Predicted results obtained by Miner rule, the proposed model and the modified model for Case 1: aluminium alloy Al-2024

Load sequence	Load stress	Experimental data				Miner rule n_2/N_{f2}	Proposed model n_2/N_{f2}	Modified model n_2/N_{f2}
		n_1	n_1/N_{f1}	n_2	n_2/N_{f2}			
Low-high	$\sigma_1 = 150$ Mpa	86 000	0.200	144 500	0.963	0.800	0.844	0.967
	$\sigma_2 = 200$ Mpa	172 000	0.400	133 500	0.890	0.600	0.646	0.824
		258 000	0.600	81 700	0.545	0.400	0.434	0.574
High-low	$\sigma_1 = 200$ Mpa	30 000	0.200	228 700	0.532	0.800	0.753	0.578
	$\sigma_2 = 150$ Mpa	60 000	0.400	101 050	0.235	0.600	0.556	0.419
		90 000	0.600	76 050	0.177	0.400	0.369	0.277

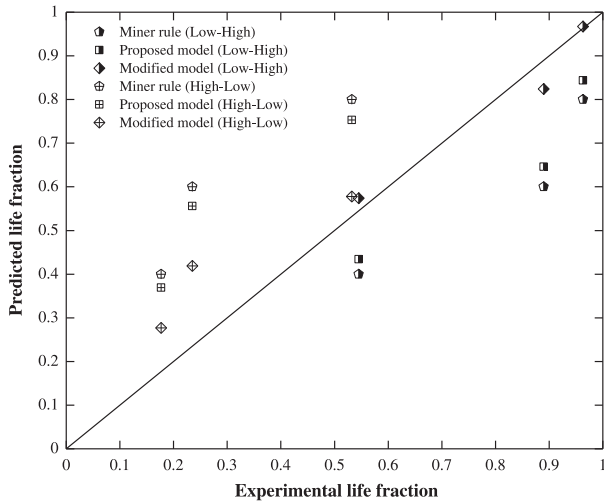


Fig. 3 Comparison of predicted results obtained by Miner rule, the proposed model and the modified model for aluminium alloy Al-2024.

high-low loading sequence, and 74–89 Mpa and 74–104 Mpa for low-high loading sequence; fatigue lives for these three applied stresses $\sigma = 104$ Mpa, $\sigma = 89$ Mpa and $\sigma = 74$ Mpa are $N_f = 549\,300$ cycles, $N_f = 880\,500$ cycles and $N_f = 1\,540\,100$ cycles, respectively. For fillet weld joint, the tests were also carried out under two-level block loading, including low-high and high-low loading sequences; three applied stress levels are $\sigma = 93$ Mpa, $\sigma = 83$ Mpa, and $\sigma = 73$ Mpa and their fatigue lives are $N_f = 619\,800$ cycles, $N_f = 952\,300$ cycles and $N_f = 1\,546\,100$ cycles, respectively; four configurations of load spectrums are 93–73 Mpa and 83–73 Mpa under high-low loading, and 73–83 Mpa and 73–93 Mpa under low-high loading, respectively.

The original data from experiments and theoretical results obtained by Miner rule, the proposed model and the modified model are listed in Table 2. It shows that all the predictions from the proposed model and the modified model are consistent with the experimental results. For

Table 2 Predicted results obtained by three models for Case 2: butt weld joint and fillet weld joint

Type of weld joint	Load sequence	Load stress	Experimental data				Miner rule n_2/N_{f2}	Proposed model n_2/N_{f2}	Modified model n_2/N_{f2}	
			$n_1 / 10^3$	n_1 / N_{f1}	$n_2 / 10^3$	n_2 / N_{f2}				
Butt weld joint	High-low	$\sigma_1 = 104$ Mpa $\sigma_2 = 74$ Mpa	109.9	0.200	797.6	0.518	0.800	0.752	0.541	
		$\sigma_1 = 89$ Mpa $\sigma_2 = 74$ Mpa	176.1	0.200	1029.2	0.668	0.800	0.774	0.651	
	Low-high	$\sigma_1 = 74$ Mpa $\sigma_2 = 89$ Mpa	770.1	0.500	545.6	0.620	0.500	0.520	0.623	
		$\sigma_1 = 74$ Mpa $\sigma_2 = 104$ Mpa	770.1	0.500	418.9	0.763	0.500	0.538	0.746	
	Fillet weld joint	High-low	$\sigma_1 = 93$ Mpa $\sigma_2 = 73$ Mpa	309.9	0.500	587.5	0.380	0.500	0.469	0.369
			$\sigma_1 = 83$ Mpa $\sigma_2 = 73$ Mpa	476.1	0.500	681.1	0.441	0.500	0.484	0.426
Low-high		$\sigma_1 = 73$ Mpa $\sigma_2 = 83$ Mpa	509.2	0.329	708.2	0.744	0.671	0.691	0.774	
		$\sigma_1 = 73$ Mpa $\sigma_2 = 93$ Mpa	773.0	0.500	426.4	0.688	0.500	0.532	0.670	

each weld joint, both of the presented models always give $n_1/N_{f1} + n_2/N_{f2} > 1$ for low–high loading sequence and $n_1/N_{f1} + n_2/N_{f2} < 1$ for high–low loading sequence. In addition, a graph comparison of the experimental data and predictions are illustrated in Fig. 4. Note that the proposed model gives better predictions than the Miner rule, while the modified model shows a better correlation between the theoretical and experimental results than the others.

Case 3: spheroidal graphite cast-iron (GS61)

The material studied here in this case is spheroidal graphite cast-iron (GS61).⁷ Two types of loading tests, plane bending and torsion, were also performed under two-

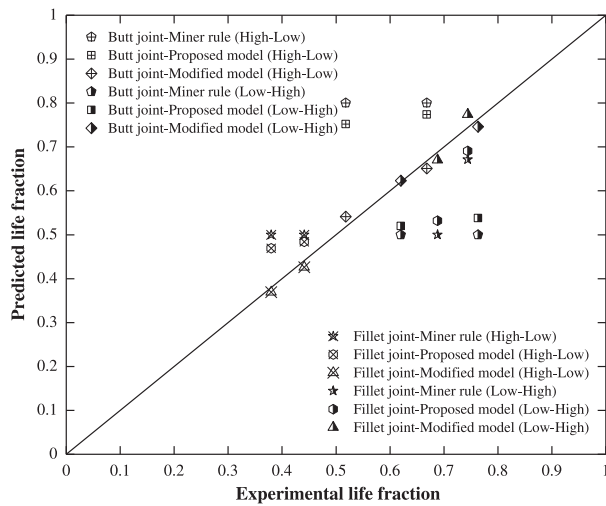


Fig. 4 Comparison of predicted results obtained by Miner rule, the proposed model and the modified model for butt weld joint and fillet weld joint.

level block loading for both low–high and high–low loading sequences. For plane bending loading, three applied stress levels are $\sigma = 352$ Mpa, $\sigma = 320$ Mpa, and $\sigma = 303$ Mpa and their fatigue lives are $N_f = 112\,847$ cycles, $N_f = 322\,580$ cycles, $N_f = 588\,235$ cycles, respectively; four combinations of load spectrums are 320–352 Mpa and 303–352 Mpa for low–high loading sequence, and 352–320 Mpa and 352–303 Mpa for high–low loading sequence, respectively. For torsion loading, two applied stress levels are $\sigma = 249$ Mpa and $\sigma = 233$ Mpa, and their fatigue lives are $N_f = 119\,904$ cycles, and $N_f = 299\,065$ cycles, respectively; load spectrums under low–high and high–low loading sequence are 233–249 Mpa and 249–233 Mpa, respectively.

In Table 3, it shows the details of experimental data and predicted results using Miner rule, the proposed model and the modified model. The proposed model, as well as the modified model, again follows the trend in that $n_1/N_{f1} + n_2/N_{f2} > 1$ for low–high loading sequence and $n_1/N_{f1} + n_2/N_{f2} < 1$ for high–low loading sequence. Also, most predictions from these two presented models are close to the experimental results, only one observation deviates from experimental value, which occurs in the torsion test under low–high loading sequence. Besides, in Fig. 5, it clearly displays the differences between the experimental data and predictions. It is worth noting that the calculation results using the proposed model are better than those using the Miner rule, while the modified model gives reasonably accurate predictions in contrast with the others.

Case 4: aluminium alloy 6082T6

The material used in the current study is aluminium alloy 6082T6.^{7,30} The experiments were conducted under four-level block loading with three different

Table 3 Predicted results of three models for Case 3: spheroidal graphite cast-iron (GS61)

Type of loading	Load sequence	Load stress	Experimental data				Miner rule n_2/N_{f2}	Proposed model n_2/N_{f2}	Modified model n_2/N_{f2}
			n_1	n_1/N_{f1}	n_2	n_2/N_{f2}			
Plane bending	Low–high	$\sigma_1 = 320$ Mpa	110 000	0.341	82 830	0.734	0.659	0.681	0.725
		$\sigma_2 = 352$ Mpa							
	High–low	$\sigma_1 = 303$ Mpa	160 000	0.272	116 650	1.030	0.728	0.759	0.824
		$\sigma_2 = 352$ Mpa							
Torsion	Low–high	$\sigma_1 = 352$ Mpa	50 000	0.443	130 510	0.405	0.557	0.535	0.494
		$\sigma_2 = 320$ Mpa							
	High–low	$\sigma_1 = 352$ Mpa	50 000	0.443	205 040	0.349	0.557	0.522	0.459
		$\sigma_2 = 303$ Mpa							
Torsion	Low–high	$\sigma_1 = 233$ Mpa	160 000	0.535	46 310	0.386	0.465	0.480	0.602
	High–low	$\sigma_1 = 249$ Mpa	50 000	0.417	154 270	0.516	0.583	0.567	0.513
		$\sigma_2 = 233$ Mpa							

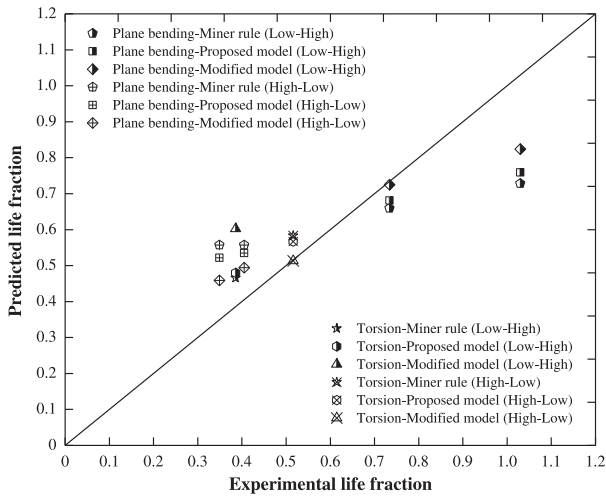


Fig. 5 Comparison of predicted results obtained by Miner rule, the proposed model and the modified model for spheroidal graphite cast-iron (GS61).

loading sequences (increasing, decreasing and irregular loading sequence). Four applied stress levels were considered, i.e. $\sigma = 240$ Mpa, $\sigma = 260$ Mpa, $\sigma = 280$ Mpa and $\sigma = 305$ Mpa, and their fatigue lives are $N_f = 394\,765$ cycles, $N_f = 180\,660$ cycles, $N_f = 87\,612$ cycles and $N_f = 38\,000$ cycles, respectively. Load spectrums for increasing, decreasing and irregular loading sequence are 240–260–280–305 Mpa, 305–280–260–240 Mpa and 280–305–260–240 Mpa, respectively.

A detailed overview of experimental data and predicted results from Miner rule, the proposed model and the modified model is shown in Table 4. It seems that the predictions of these two presented models closely accord with the experimental data; once again they still follow the same trend in that $n_1/N_{f1} + n_2/N_{f2} + n_3/N_{f3} + n_4/N_{f4} > 1$ for low–high loading sequence

and $n_1/N_{f1} + n_2/N_{f2} + n_3/N_{f3} + n_4/N_{f4} < 1$ for high–low loading sequence. In addition, a comparison between the experimental data and models predictions is represented in Fig. 6. Obviously, the predicted life fractions by the proposed model match well with the experimental results, compared with those of the Miner rule, while the modified model yields better results than the others.

Case 5: titanium alloy Ti–6Al–4V

The material of titanium alloy Ti–6Al–4V is studied in this case.⁴³ The experiments were performed with three configurations of two-level block loading, i.e. high–low, low–high and repeated block loading. For these three loading tests, the applied higher and lower stress levels are $\sigma = 217$ Mpa and $\sigma = 121$ Mpa, and their average fa-

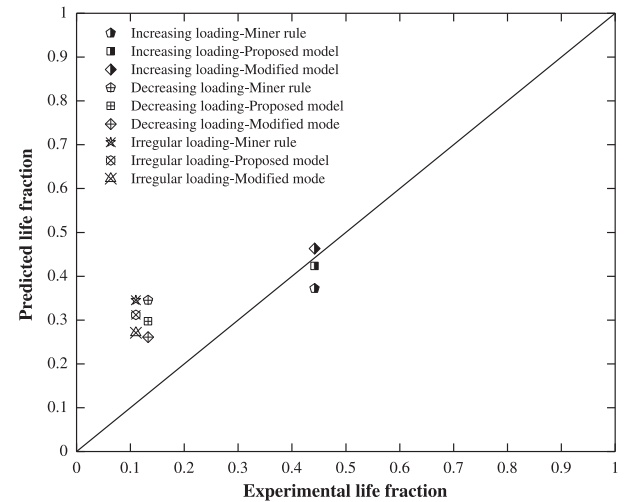


Fig. 6 Comparison of predicted results obtained by Miner rule, the proposed model and the modified model for aluminium alloy 6082T6.

Table 4 Predicted results of three models for Case 4: aluminium alloy 6082T6

Block	Experimental data				Miner rule	Proposed model	Modified model
	1	2	3	4			
01 Increasing loading							
Load stress (Mpa)	240	260	280	305			
<i>n</i> cycles	103 000	26 256	19 427	16 800	14 136	16 074	17 594
n/N_f	0.261	0.145	0.222	0.442	0.372	0.423	0.463
02 Decreasing loading							
Load stress (Mpa)	305	280	260	240			
<i>n</i> cycles	10 950	19 427	26 258	52 500	136 190	117 250	103 030
n/N_f	0.288	0.222	0.145	0.133	0.345	0.297	0.261
03 Irregular loading							
Load stress (Mpa)	280	305	260	240			
<i>n</i> cycles	19 427	10 950	26 258	43 400	136 190	123 170	106 980
n/N_f	0.222	0.288	0.145	0.110	0.345	0.312	0.271

tigue lives are $N_f=82\,968$ cycles and $N_f=371\,944$ cycles, respectively. Load spectrums under high–low and low–high loading are 217–121 Mpa and 121–217 Mpa, respectively. In the repeated two-level block loading, each block is taken as a high–low loading (217–121 Mpa) with various combinations of specified fatigue cycles for these two stress levels.

Loading conditions, experimental data and model predictions are listed in Table 5 (M_f denotes the number of repeated blocks to fracture, $M_f=1$ for the two-level high–low and low–high block loading). In the table, it can be found that the calculation results using the proposed rules conform to the experimental data; both of them yield $M_f n_1 / N_{f1} + M_f n_2 / N_{f2} > 1$ for low–high loading and $M_f n_1 / N_{f1} + M_f n_2 / N_{f2} < 1$ for high–low loading and repeated block loading. To clearly show these results, plots of the life fraction $M_f n_2 / N_{f2}$ versus the life fraction $M_f n_1 / N_{f1}$ are shown in Fig. 7 (Exp. and Pre. denote the experimental data and predictions, respectively). It is observed that the predictions of the Miner rule show a significant discrepancy with the experimental data; the modified model yields a better correlation between the theoretical and experimental results than the proposed model.

DISCUSSIONS

According to the five above-mentioned case studies, it shows that the proposed model and the modified model predict that the sum of life fractions with the increasing

loading is greater than 1, while the decreasing loading is less than 1. This phenomenon agrees with many experimental evidences, suggesting that the damage mechanisms responsible for variable fatigue loading have a strong dependence of load sequences. The proposed non-linear rules are capable of producing different CAL damage functions (the cumulative damage D in relation to the consumed life fraction n/N_f), which depends on the applied loads. Using the equivalent damage rule, it

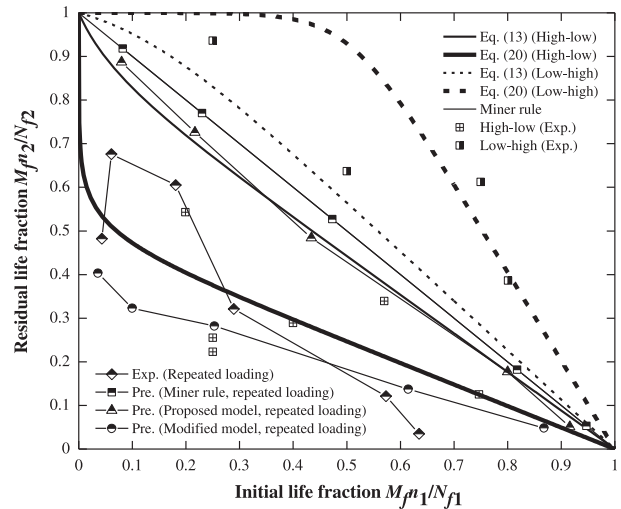


Fig. 7 Plots of the life fraction $M_f n_2 / N_{f2}$ versus the life fraction $M_f n_1 / N_{f1}$ under three configurations of two-level block loading for titanium alloy Ti–6Al–4V.

Table 5 Predicted results obtained by three models for Case 5: titanium alloy Ti–6Al–4V

Load stress	Experimental data				Miner rule		Proposed model		Modified model	
	n_1	n_2	$M_f n_1 / N_{f1}$	$M_f n_2 / N_{f2}$	$M_f n_1 / N_{f1}$	$M_f n_2 / N_{f2}$	$M_f n_1 / N_{f1}$	$M_f n_2 / N_{f2}$	$M_f n_1 / N_{f1}$	$M_f n_2 / N_{f2}$
Two-level high–low block loading										
$\sigma_1 = 217$ Mpa	16 500	202 145	0.199	0.543	0.199	0.801	0.199	0.720	0.199	0.405
$\sigma_2 = 121$ Mpa	20 740	94 951	0.250	0.255	0.250	0.750	0.250	0.670	0.250	0.376
	20 740	82 900	0.250	0.223	0.250	0.750	0.250	0.670	0.250	0.376
	33 210	107 566	0.400	0.289	0.400	0.600	0.400	0.532	0.400	0.297
	47 300	126 142	0.570	0.339	0.570	0.430	0.570	0.380	0.570	0.212
	62 000	46 440	0.747	0.125	0.747	0.253	0.747	0.224	0.747	0.125
Two-level low–high block loading										
$\sigma_1 = 121$ Mpa	93 000	77 646	0.250	0.936	0.250	0.750	0.250	0.830	0.250	0.999
$\sigma_2 = 217$ Mpa	186 000	52 863	0.500	0.637	0.500	0.500	0.500	0.565	0.500	0.930
	279 000	50 745	0.750	0.612	0.750	0.250	0.750	0.283	0.750	0.506
	298 000	32 000	0.801	0.386	0.801	0.199	0.801	0.225	0.801	0.404
Repeated two-level block loading										
$\sigma_1 = 217$ Mpa	300	15 000	0.043	0.482	0.082	0.918	0.080	0.887	0.036	0.403
$\sigma_2 = 121$ Mpa	300	15 000	0.061	0.676	0.082	0.918	0.080	0.887	0.036	0.403
	1000	15 000	0.181	0.605	0.230	0.770	0.217	0.726	0.100	0.323
	3000	15 000	0.289	0.321	0.473	0.527	0.434	0.484	0.253	0.282
	3000	3000	0.573	0.121	0.818	0.182	0.800	0.177	0.615	0.137
	4000	1000	0.635	0.035	0.947	0.053	0.916	0.051	0.868	0.048

leads to different Miner's damage sums for different loading sequences. The proposed model, as well as its modifications, shows a better agreement between the predicted and experimental results than the Miner rule whatever the loading configuration. Among these three models, Miner rule still dominantly used has the simplest form and is easy to implement in design. However, the model does not take into account loading histories (such as load sequences and load interactions). The function formulating the CAL fatigue damage with respect to n/N_f is independent of applied loads, while it has been verified that fatigue failure for many metallic materials commonly exhibits highly non-linear damage behaviours with load dependency.^{44,45} Therefore, the predictions using Miner rule do not strongly correlate with the experimental results.

Compared with the Miner rule, the proposed model of Eq. 12 yields a non-linear damage behaviour dependent on the fatigue life of applied load, showing the effects of load sequences under VAL. Thus, the model is expected to give lower deviations than Miner rule. In the present work, the proposed model is developed based on the concept of fatigue driving energy. The parameter is exhibited as a combination of the fatigue driving stress and strain energy density. For the proposed model, it assumes that fatigue damage variable D is defined by assessing the change of FDE. The model can not only remedy the insufficiency associated with fatigue driving stress model (σ_{equiv} should be available in Fig. 1) but also provide clear physical connotations. It is the FDE driving fatigue damage with the consumed life fraction n/N_f gradually. At $n/N_f=0$, the initial FDE is just dependent on the applied stress, attempting to cause damage in the material, and the cumulative damage $D=0$; thereafter, the FDE, as well as the cumulative damage, will increase non-linearly with the accumulated cycles, and $D>0$, indicating that the material is damaged progressively; when $n/N_f=1$, the FDE reaches a threshold, treated as the inherent energy stored in material for preventing the material from failure, the complete fracture occurs, and $D=1$. As a consequence, the proposed model offers an appropriate method to characterize the complete process of fatigue failure. However, it is found that the predictions of this model are slightly better than the counterparts by Miner rule. This suggests that the damage evolution under VAL may become very complicated. Although the proposed model can deal with the load sequence effects, the damage evolution law of variable fatigue loading can be dominated by other effects because of the complex loading histories, such as load interactions.

In addition, the modified model exhibits a better prediction performance than the others. On the basis of the proposed model, its modifications are designed to

consider the effects of load interaction. In Eq. 19, it suggests a possible way to assess the effects between two successive stress levels on damage accumulation. Owing to incorporating the effects of load sequence and load interaction, the predictions using these modifications can correctly follow the experimental results and are more representative than those of the proposed model and Miner rule.

Moreover, for titanium alloy Ti-6Al-4V, as illustrated in Fig. 7, the proposed model, as well as its modification, yields different fatigue envelopes for different loading sequences, while Miner rule yields the same envelope (a straight line). This once again suggests that Miner rule is load order independent and fails to consider this effect on damage accumulation; the proposed rules have the capability of producing load sequences. The high-low envelope and low-high envelope are symmetric with respect to the Miner's envelope, and all of envelopes are confined by the box from (0, 0) to (1, 1). Hence, this case can demonstrate the typical behaviours of the proposed non-linear rules. For the case of two-level block loadings, as shown in Table 5, the fatigue envelopes using the modified model are in a better agreement with the experimental data than those of the proposed rule and Miner rule, because of the consideration of load interaction effects. In the repeated block loading, note that the modified rule achieves better prediction accuracy than the others. This modification allows us to consider more load histories information and to give reasonable predictions, in spite of the complex fatigue behaviour under such repeated loading. Consequently, the modified rule can be used to estimate the fatigue life under repeated block loading conditions.

Furthermore, the newly proposed models still maintain a simple form and are easy to be implemented based on the S-N curve. Both of them are only applicable to high-cycle fatigue regime under uniaxial loading and can be extended to multi-axial loading. At present, the new rules developed are based on deterministic methodology, while variable fatigue loading is often involved in various uncertainties and exhibits highly complexities. Hence, life prediction associated with these uncertainties remains to be investigated, aiming to provide an accurate assessment.

CONCLUSIONS

In this study, a concept of fatigue driving energy is presented as a combination of the fatigue driving stress and strain energy density to characterize the fatigue damage. By assessing the change of FDE parameter, a non-linear damage model is developed for high-cycle fatigue life

prediction under VAL. This new model offers the possibility of describing the complete process of fatigue failure. Through comparing it with the Miner rule, the model shows lesser deviations with the reality and can correctly describe the effects of load sequence responsible for variable fatigue loading.

Through taking the load interaction effects into account, a modification based on the proposed model is also developed and further improves its prediction accuracy. The typical behaviours of these two presented non-linear rules under two-level block loading are demonstrated by the case of titanium alloy Ti-6Al-4V. The models properties are also verified and the modified rule can be applied to the repeated block loading. Moreover, both of the new rules maintain a simple form and are ease of application by using the S-N curve only.

Acknowledgements

The present study was partially supported by the National Natural Science Foundation of China under the contract number 11272082.

REFERENCES

- 1 Miner, M. A. (1945) Cumulative damage in fatigue. *J. Appl. Mech.*, **12**, 159–164.
- 2 Schijve, J. (2001) *Fatigue of Structures and Materials*. Kluwer Academic: Dordrecht.
- 3 Fatemi, A. and Yang, L. (1998) Cumulative fatigue damage and life prediction theories: a survey of the state of the art for homogeneous materials. *Int. J. Fatigue*, **20**, 9–34.
- 4 Manson, S. S. and Halford, G. R. (1986) Re-examination of cumulative fatigue damage analysis—an engineering perspective. *Eng. Fract. Mech.*, **25**, 539–571.
- 5 Mesmacque, G., Garcia, S., Amrouche, A. and Rubio-Gonzalez, C. (2005) Sequential law in multiaxial fatigue, a new damage indicator. *Int. J. Fatigue*, **27**, 461–467.
- 6 Colin, J. and Fatemi, A. (2010) Variable amplitude cyclic deformation and fatigue behaviour of stainless steel 304L including step, periodic, and random loadings. *Fatigue Fract. Eng. Mater. Struct.*, **33**, 205–220.
- 7 Aid, A., Amrouche, A., Bouiadjra, B. B., Benguediab, M. and Mesmacque, G. (2011) Fatigue life prediction under variable loading based on a new damage model. *Mater. Des.*, **32**, 183–191.
- 8 Yuan, R., Li, H., Huang, H. Z., Zhu, S. P. and Li, Y. F. (2013) A new non-linear continuum damage mechanics model for fatigue life prediction under variable loading. *Mech. Mater.*, **19**, 506–511.
- 9 Yang, X. H., Yao, W. X. and Duan, C. M. (2003) The development of deterministic fatigue cumulative damage theory. *Eng. Sci.*, **5**, 81–87.
- 10 Zhu, S. P., Huang, H. Z. and Wang, Z. L. (2011) Fatigue life estimation considering damaging and strengthening of low amplitude loads under different load sequences using Fuzzy sets approach. *Int. J. Damage Mech.*, **20**, 876–899.
- 11 Liakat, M. and Khonsari, M. M. (2014) An experimental approach to estimate damage and remaining life of metals under uniaxial fatigue loading. *Mater. Des.*, **57**, 289–297.
- 12 Belaadi, A., Bezazi, A., Bourchak, M. and Scarpa, F. (2013) Tensile static and fatigue behaviour of sisal fibres. *Mater. Des.*, **46**, 76–83.
- 13 Zhou, Y., Jerrams, S. and Chen, L. (2013) Multi-axial fatigue in magnetorheological elastomers using bubble inflation. *Mater. Des.*, **50**, 68–71.
- 14 Ye, D. Y. and Wang, Z. L. (2001) A new approach to low-cycle fatigue damage based on exhaustion of static toughness and dissipation of cyclic plastic strain energy during fatigue. *Int. J. Fatigue*, **23**, 679–687.
- 15 Devulder, A., Aubry, D. and Puel, G. (2010) Two-time scale fatigue modelling: application to damage. *Comput. Mech.*, **45**, 637–646.
- 16 Cheng, G. and Plumtree, A. (1998) A fatigue damage accumulation model based on continuum damage mechanics and ductility exhaustion. *Int. J. Fatigue*, **20**, 495–501.
- 17 Zhu, S. P., Huang, H. Z., Liu, Y., Yuan, R. and He, L. (2013) An efficient life prediction methodology for low cycle fatigue-creep based on ductility exhaustion theory. *Int. J. Damage Mech.*, **22**, 556–571.
- 18 Zhu, S. P., Huang, H. Z. and Xie, L. Y. (2008) Non-linear fatigue damage cumulative model and the analysis of strength degradation based on the double parameter fatigue criterion. *China Mech. Eng.*, **19**, 2753–2761.
- 19 Yuan, R., Li, H., Huang, H. Z., Zhu, S. P. and Gao, H. (2014) A non-linear fatigue damage accumulation model considering strength degradation and its applications to fatigue reliability analysis. *Int. J. Damage Mech.*, DOI: 10.1177/1056789514544228.
- 20 Lemaitre, J. and Dufailly, J. (1987) Damage measurements. *Eng. Fract. Mech.*, **28**, 643–661.
- 21 Sun, B., Yang, L. and Guo, Y. (2007) A high-cycle fatigue-accumulation model based on electrical resistance for structural steels. *Fatigue Fract. Eng. Mater. Struct.*, **30**, 1052–1062.
- 22 Naderi, M. and Khonsari, M. M. (2010) A thermodynamic approach to fatigue damage accumulation under variable loading. *Mater. Sci. Eng. A*, **527**, 6133–6139.
- 23 Amiri, M. and Khonsari, M. M. (2012) On the role of entropy generation in processes involving fatigue. *Entropy*, **14**, 24–31.
- 24 Khonsari, M. M. and Amiri, M. (2013) *Introduction to Thermodynamics of Mechanical Fatigue*. CRC Press Florida.
- 25 Azari, Z., Lebienu, M. and Pluvinage, G. (1984) Functions of damage in low-cycle fatigue. *Adv. Fract. Res.*, **3**, 1815–1821.
- 26 Azadi, M., Farrahi, G. H., Winter, G. and Eichlseder, W. (2014) Fatigue lifetime of AZ91 magnesium alloy subjected to cyclic thermal and mechanical loadings. *Mater. Des.*, **53**, 639–644.
- 27 Łagoda, T. (2001) Energy models for fatigue life estimation under uniaxial random loading. Part I: the model elaboration. *Int. J. Fatigue*, **23**, 467–480.
- 28 Łagoda, T. (2001) Energy models for fatigue life estimation under uniaxial random loading. Part II: verification of the model. *Int. J. Fatigue*, **23**, 481–489.
- 29 Park, S. H., Hong, S. G., Lee, B. H. and Lee, C. S. (2008) Fatigue life prediction of rolled AZ31 magnesium alloy using an energy-based model. *Int. J. Mod. Phys. B*, **22**, 5503–5508.
- 30 Djebli, A., Aid, A., Bendouba, M., Amrouche, A., Benguediab, B. and Benseddiq, N. (2013) A non-linear energy model of fatigue damage accumulation and its verification for Al-2024 aluminum alloy. *Int. J. Non-linear Mech.*, **51**, 145–151.
- 31 Zhu, S. P., Huang, H. Z., He, L., Liu, Y. and Wang, Z. (2012) A generalized energy-based fatigue-creep damage parameter for

- life prediction of turbine disk alloys. *Eng. Fract. Mech.*, **90**, 89–100.
- 32 Kwofie, S. and Rahbar, N. (2013) A fatigue driving stress approach to damage and life prediction under variable amplitude loading. *Int. J. Damage Mech.*, **22**, 393–404.
- 33 Richart, F. E. and Newmark, N. M. (1948) A hypothesis for the determination of cumulative damage in fatigue. *Am. Soc. Test. Mater. Proc.*, **48**, 767–800.
- 34 Freudenthal, A. M. and Heller, R. A. (1959) On stress interaction in fatigue and cumulative damage rule. *J. Aerospace Sci.*, **26**, 431–442.
- 35 Morrow, J. D. (1986) The effect of selected sub-cycle sequences in fatigue loading histories. *Random Fatigue Life Predictions, ASME Publication PVP*, **72**, 43–60.
- 36 Skorupa, M. (1998) Load interaction effects during fatigue crack growth under variable amplitude loading—a literature review. Part I: empirical trends. *Fatigue Fract. Eng. Mater. Struct.*, **21**, 987–1006.
- 37 Skorupa, M. (1999) Load interaction effects during fatigue crack growth under variable amplitude loading—a literature review. Part II: qualitative interpretation. *Fatigue Fract. Eng. Mater. Struct.*, **22**, 905–926.
- 38 Lv, Z., Huang, H. Z., Zhu, S. P., Gao, H. and Zuo, F. (2014) A modified nonlinear fatigue damage accumulation model. *Int. J. Damage Mech.*, **24**, 168–181.
- 39 Corten, H. T. and Dolan, T. J. (1956) Cumulative fatigue damage. *Proc. Int. Conf. on Fatigue of Metals, Institution of Mechanical Engineers, London*, 235–246.
- 40 Gao, H., Huang, H. Z., Zhu, S. P., Li, Y. F. and Yuan, R. (2014) A modified nonlinear damage accumulation model for fatigue life prediction considering load interaction effects. *Sci. World J.*, Article ID 164378, 7 pages, 10.1155/2014/164378.
- 41 Pavlou, D. G. (2002) A phenomenological fatigue damage accumulation rule based on hardness increasing, for the 2024-T42 aluminum. *Eng. Struct.*, **24**, 1363–1368.
- 42 Tian, J., Liu, Z. M. and He, R. (2012) Non-linear fatigue-cumulative damage model for welded aluminum alloy joint of EMU. *J. China Railw. Soc.*, **34**, 40–43.
- 43 Jin, O., Lee, H. and Mall, S. (2003) Investigation into cumulative damage rules to predict fretting fatigue life of Ti–6Al–4V under two-level block loading condition. *J. Eng. Mater. Tech.*, **125**, 315–323.
- 44 Jono, M. (2005) Fatigue damage and crack growth under variable amplitude loading with reference to the counting methods of stress–strain ranges. *Int. J. Fatigue*, **27**, 1006–1015.
- 45 Aghoury, I. E. and Galal, K. (2013) A fatigue stress-life damage accumulation model for variable amplitude fatigue loading based on virtual target life. *Eng. Struct.*, **52**, 621–628.